

Drip line to drip line microscopic nuclear level densities

Hilaire S.*

CEA, DAM, DIF, F-91297, Arpajon, France

Goriely S.

*Institut d'Astronomie et d'Astrophysique, Université Libre de Bruxelles,
Campus de la Plaine CP226, 1050 Brussels, Belgium*

Koning A.J.

Nuclear Research and Consultancy Group, P.O. Box 25, NL-1755 ZG Petten, The Netherlands

(Dated: February 9, 2009)

New developments have been brought to our previously calculated energy-, spin- and parity-dependent nuclear level densities based on the microscopic combinatorial model [1]. Like in our previous study, a detailed calculation of the intrinsic state density and of rotational enhancement factor is included, but this time the vibrational contributions explicitly take the phonon excitations into account using a vibrational partition function instead of a phenomenological enhancement factor. This new model predicts the experimental s- and p-wave neutron resonance spacings with a degree of accuracy comparable to that of the best global models available and also provides reasonable description of low energies cumulative number of levels. The predictions are also in good agreement with experimental data obtained by the Oslo group [2]. Total as well as partial level densities for more than 8500 nuclei are made available in a table format for practical applications, and for the nuclei for which experimental s-wave spacings and enough low-lying states exist, renormalization factors are also provided to reproduce simultaneously both observables.

I. INTRODUCTION

The knowledge of nuclear level densities (NLDs) has been a matter of interest and study for years going back at least to 1936 with Bethe's pioneering work [3]. Since then, more or less sophisticated methods have been developed to reproduce the available experimental data. The so-called partition function method is by far the most widely used technique to calculate level densities. It corresponds to the zeroth order approximation of a Fermi gas model and leads to more or less simple analytical expressions depending on parameters which are generally adjusted to reproduce scarce experimental data [4–7]. However, in specific applications such as nuclear astrophysics or accelerator-driven systems, a large number of data needs to be obtained far away from the experimentally known region. In this case, two major features of the nuclear theory must be contemplated, namely its *reliability* and *accuracy*. A microscopic description by a physically sound model based on first principles ensures a reliable extrapolation away from experimentally known region. For these reasons, when no experimental data exists to constrain analytical Fermi-gas-type formulae, it is imperative to use preferentially microscopic or semi-microscopic global predictions based on sound and reliable nuclear models which, in turn, can compete with more phenomenological highly-parameterized models in the reproduction of experimental data. Global microscopic models of NLD have been developed for the last

decades [8–14], but they are almost never used for practical applications, because of their lack of accuracy in reproducing experimental data (especially when considered globally on a large data set) or because they do not offer the same flexibility as that of the highly parametrized analytical expressions.

A global microscopic NLD prescription within the statistical approach based on the Hartree-Fock-BCS (HF-BCS) ground state properties [15] has proven the capacity of microscopic models to compete with phenomenological models in the reproduction of experimental data and consequently to be adopted for practical applications. However, this statistical approach presents the drawback of not describing the parity dependence of the NLD, nor the discrete (i.e non-statistical) nature of the excited spectrum at low energies. For this reason, we recently improved the combinatorial approach and demonstrated that such an approach can clearly compete with the statistical approach in the global reproduction of experimental data [1]. One of the advantages of this approach is to provide not only the energy, spin and parity dependence of the NLD, but also the partial particle-hole level density that cannot be extracted in any satisfactory way from the statistical approaches. At low energies, the combinatorial predictions also provide the non-statistical limit where by definition the statistical approach cannot be applied.

II. THE COMBINATORIAL METHOD

Our method consists in using the single-particle level schemes obtained from constrained axially symmetric

*Electronic address: stephane.hilaire@cea.fr

Hartree-Fock-Bogoliubov (HFB) method to construct incoherent particle-hole (ph) state densities as functions of the excitation energy, the spin projection (on the intrinsic symmetry axis of the nucleus) and the parity. Once these incoherent ph state densities are determined, collective effects have to be included. In [1], the choice was made to describe the vibrational effects by multiplying the total level densities by a phenomenological enhancement factor described in [6, 7] once rotational bands had been constructed. The resulting nuclear level densities were found to reproduce very well the available experimental data (i.e. both the cumulated low energy discrete level histograms and the s- and p-wave resonances mean spacings at the neutron binding energy). However, it is clear that the phenomenological treatment of vibrational effects needs to be replaced by a sounder treatment. Indeed, rotational bands built on purely vibrational band-heads are well established and can clearly not be described if the vibrational enhancement occur once the rotational bands are constructed as done in [1]. Feedback from fission cross section calculations also suggested this lack of vibrational states at low energies [16]. To improve the reliability of the microscopic prediction of NLD, the vibrational enhancement factor is now included in the combinatorial approach explicitly by allowing for phonon excitations using the boson partition function of ref. [13] which includes quadrupole, octupole as well as hexadecapole vibrational modes. Whereas single-particle levels are theoretically obtained for any nucleus, phonon's energies are taken from experimental information when available or from analytical expressions [17]. Once the vibrational and incoherent ph state densities are computed, they are folded to deduce the total state and the level densities are then deduced exactly like in [1]. To account for the damping of vibrational effects at increasing energies, we restrict the folding to the ph configurations having a total exciton number (i.e. the sum of the number of proton and neutron particles and proton and neutron holes) $N_{ph} \leq 4$. This restriction stems from the fact that a vibrational state results from a coherent excitation of particles and holes, and that this coherence vanishes with increasing number of ph involved in the description. Therefore, if one deals with a ph configuration having a large exciton number, one should not simultaneously account for vibrational states which are clearly already included as incoherent excitations.

III. LEVEL DENSITY RESULTS

The new NLD are now compared with experimental data. In spite of considerable experimental efforts made to derive NLD, the lack of reliable data—especially over a wide energy range—constitutes the main problem that the NLD theories have to face. Nevertheless, a large number of analysis of slow neutron resonances and of cumulative numbers of low energy levels have greatly helped to provide experimental information on NLD. Other sources of

information have also been suggested, such as analysis of spectra of evaporated particles and coherence widths of cross section fluctuations. However, most of these experimental data are affected by systematic errors resulting from experimental uncertainties as well as the use of approximate theories to analyze them.

The most extensive and reliable source of experimental information on NLD remains the s- and p-wave neutron resonance spacings [7, 18] and the observed low-energy excited levels [18]. We show in Fig. 1 the result of our HFB plus combinatorial approach with respect to experimental s- and p-wave spacings compiled in the RIPL-2 database [18].

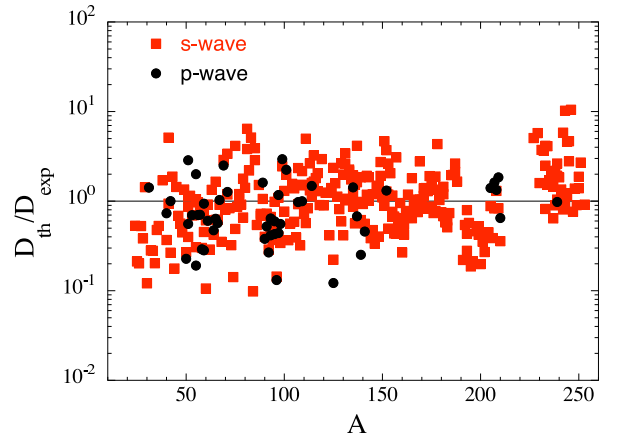


FIG. 1: Ratio of HFB plus combinatorial (D_{th}) to the experimental (D_{exp}) s-wave (squares) and p-wave (circles) neutron resonance spacings compiled in [18].

The quality of a global NLD formula can be described by the rms deviation factor defined as

$$f_{rms} = \exp \left[\frac{1}{N_e} \sum_{i=1}^{N_e} \ln^2 \frac{D_{th}^i}{D_{exp}^i} \right]^{1/2}, \quad (1)$$

where $D_{th}(D_{exp})$ is the theoretical (experimental) resonance spacing and N_e is the number of nuclei in the compilation. Globally, the D values are predicted within a factor of 2 (the exact rms factor amounts to $f_{rms} = 2.3$ for both the s- and p-wave data). This result is to be compared to the deviations of global analytical formula [4] typically of the order of 1.7 – 1.9 and the $f_{rms} = 2.14$ value obtained with our previous combinatorial result [1]. Our new approach therefore gives rather comparable predictions with respect to the other existing global models.

The HFB plus combinatorial model also gives satisfactory extrapolations to low energies. As an example, we compare in Fig. 2 the predicted cumulative number of levels $N(U)$ with the experimental data [18] for the same 15 nuclei as the one presented in [1], including light as well as heavy, spherical as well as deformed species. Globally, the present model provides similar results as those illustrated in Ref.[1].

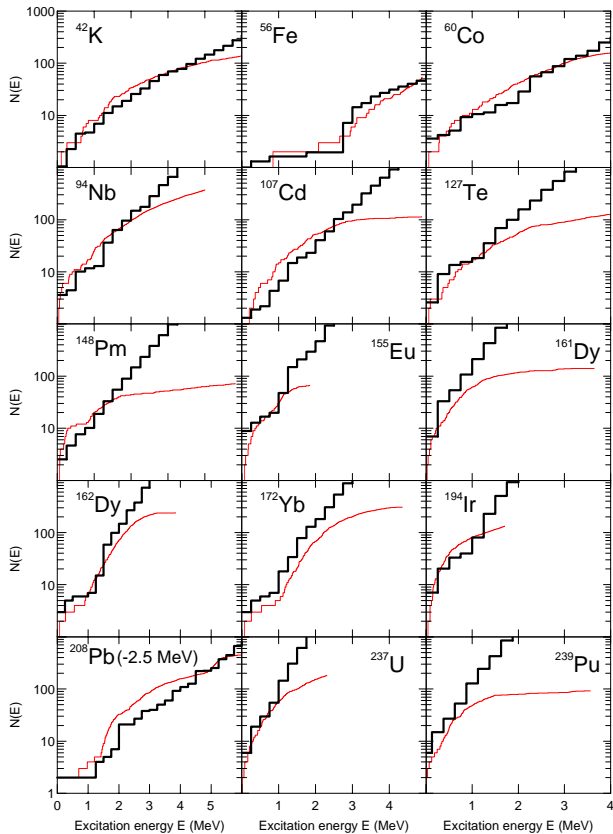


FIG. 2: Comparison of the cumulative number of observed levels (thin staircase) with the HFB plus combinatorial predictions (thick line) as a function of the excitation energy U for a sample of 15 nuclei. Only for ^{208}Pb , both curves have been shifted by 2.5 MeV, the energy range corresponding consequently to [2.5-8.5] MeV instead of [0-6] MeV.

For many nuclear physics applications a renormalization procedure of the NLD on experimental data is required, in particular for nuclear data evaluation or for an accurate and reliable estimate of reaction cross sections. Though the HFB plus combinatorial NLD are provided in a table format, it is possible to renormalize them on both the experimental level scheme at low energy and the neutron resonance spacings at $U = S_n$ in a way similar to what is usually done with analytical formulae. More specifically, the renormalized level density can be corrected through the expression

$$\rho(U, J, P)_{renorm} = e^{\alpha} \sqrt{(U-\delta)} \times \rho(U - \delta, J, P) \quad (2)$$

where the energy shift δ is essentially extracted from the analysis of the cumulative number of levels and α from the experimental s-wave neutron spacing. With such a renormalization, the experimental low-lying levels and the D_{exp} values can be reproduced reasonably well as discussed in detail in [4]. Eq.(2) has been used to fit the 289 nuclei for which both an experimental s-wave spacing (D_0) and a discrete level sequence exist. The correspond-

ing δ and α values are plotted in Fig. 3. It is important to notice that the obtained α and δ parameters show no systematic trend or A -dependence, and more particularly no correlation with shell closures. Of course, when no D_{exp} value is available, only the experimental discrete level scheme is known, so that only the δ shift is used to reproduce at best the low-lying levels.

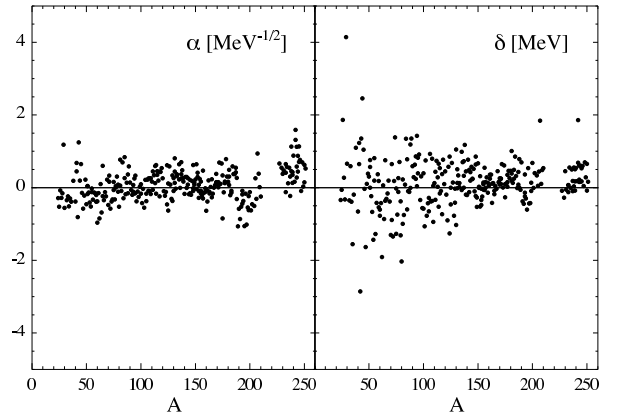


FIG. 3: α and δ values plotted as a function of the atomic mass. See text for more details.

Finally, we compare in Figs. 4 and 5, our total NLDs with the experimental data extracted by the Oslo group from the analysis of particle- γ coincidence in the ($^3\text{He}, \alpha\gamma$) and ($^3\text{He}, ^3\text{He}'\gamma$) reactions [19-27] for several isotopes. It should be stressed that such an experimental determination is however model-dependent. Indeed, in order to extract the absolute value of the total level den-

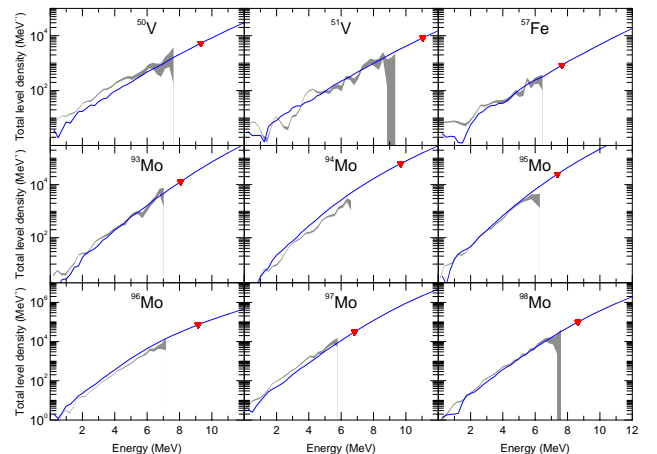


FIG. 4: Comparison between the total NLD determined by the Oslo group (Grey areas) and the HFB combinatorial predictions (solid lines). The full triangles correspond to the model-dependent normalization point derived from the D_0 value used by the Oslo group. See text for more details.

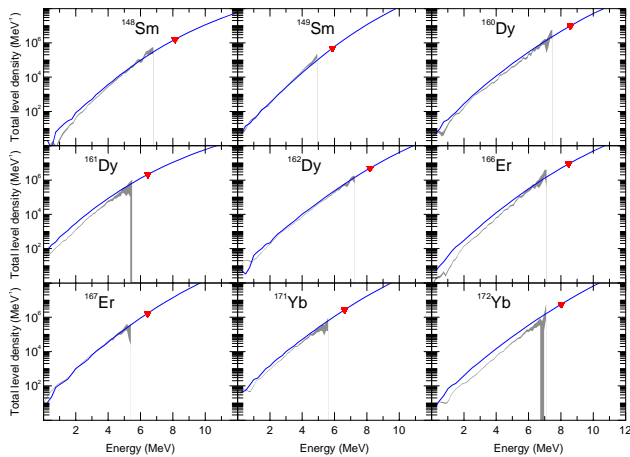


FIG. 5: Same as Fig. 4.

sity from the measured data, the so-called experimental NLD needs to be normalized by the total level density at the neutron binding energy. This normalization consists in deducing the total level density from the D_0 value, and consequently both the spin and parity distributions at the neutron binding energy are needed. If the equipartition of the parity distribution is relatively well established at these energies, discrepancies can stand from the adopted spin distribution. In particular, it is clear that a non-statistical approach such as the combinatorial method might provide different spin distributions than the simple shell- and pairing-independent Gaussian spin distribution assumed within the BSFG model and adopted by the Oslo group. Therefore, for a meaningful comparison between our predictions and the Oslo data, it is important to normalize our level densities to the level density value at $U = S_n$ considered by the Oslo group. This is done by renormalizing our predictions using Eq. (2) for each isotope, with an α parameter such that

$$\rho_{\text{HFB}}(S_n) \times \exp(\alpha \sqrt{S_n}) = \rho_{\text{oslo}}(S_n) \quad (3)$$

As can be observed, with such a normalization, the combinatorial NLD agree extremely well with the so-called experimental NLD below S_n .

IV. APPLICATION TO REACTION CROSS SECTION CALCULATIONS

In the present section, we use the HFB plus combinatorial NLD to calculate reaction cross sections with the TALYS code [28]. As an illustration, we show in Fig. 6, the specific case of the $^{89}\text{Y}(n,\gamma)^{90}\text{Y}$ cross section. The NLD predicted for ^{90}Y is shown in Fig. 6 (left panel) before and after the renormalization procedure. When the renormalization is applied (in this case to all the nuclei involved in the nuclear reaction processes), the cross

section is seen to be better described.

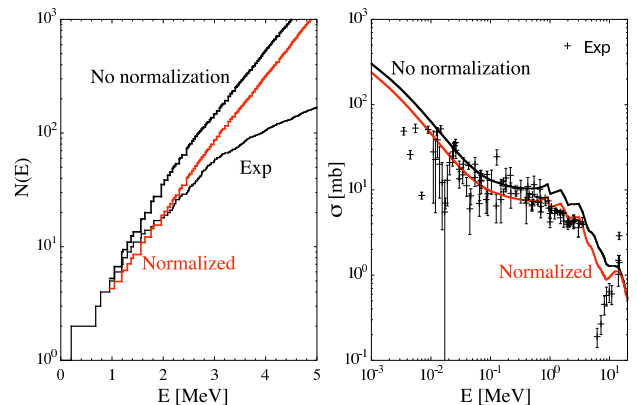


FIG. 6: Left panel : Cumulative number of levels predicted by our NLD for ^{90}Y with and without normalization. The experimental curve is shown for comparison. Right panel : $^{89}\text{Y}(n,\gamma)^{90}\text{Y}$ cross section obtained using the raw and normalized NLD and compared with experimental data [29].

In order to evaluate the overall quality of the NLD, we then compare in Fig. 7 the Maxwellian-averaged (n,γ) rates $\langle\sigma v\rangle$ at $T = 3 \times 10^8$ K with experimental data for some 219 nuclei heavier than ^{40}Ca included in the compilation of Bao et al. [30]. The radiative capture rates at such a temperature essentially reflects the cross section around a 25 keV incident neutron energy. At such energies, the radiative capture cross section is known to be very sensitive to the NLD below the neutron threshold. It appears that the calculations agree with experimental data roughly within a factor of two. Note that additional uncertainties stemming in particular from γ -ray strength functions also affect the predictions. A strong correlation between the deviations seen in the rates of Fig.7 and the NLD of Fig. 1 can be observed.

If we now use the NLD renormalized on experimental data as discussed in detail in [4] to estimate the reaction rates, the deviations with respect to experimental rates are clearly less dispersed than with the raw NLD (Fig.7). The corresponding rms deviation, based on a relation identical to Eq.(1), for the 219 nuclei is $f_{\text{rms}} = 1.92$ using the raw NLD and 1.60 with the renormalized NLD.

V. CONCLUSIONS

The combinatorial method introduced in [1] has been updated to improve the description of the collective vibrational levels. This has been performed using the boson partition function [13]. The resulting NLD are qualitatively similar to those we obtained assuming a phenomenological vibrational enhancement factor [1], both for the cumulative number of discrete levels and the mean

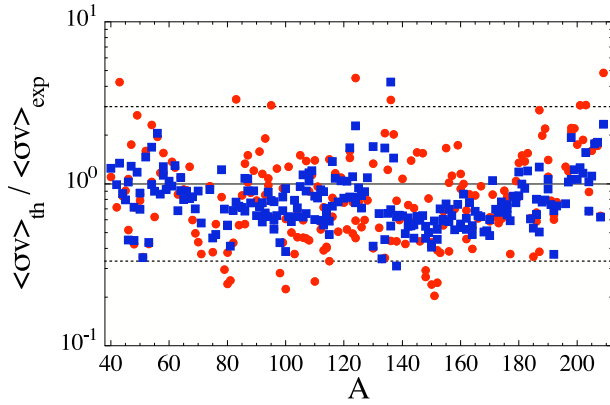


FIG. 7: Ratio of TALYS Maxwellian-averaged (n,γ) rates $\langle\sigma v\rangle_{\text{th}}$ with experimental values [30] at $T = 3 \times 10^8 \text{K}$ obtained using the raw NLD (circles) and those normalized (squares) according to the method mentioned in Sect. III.

s- and p- wave resonance spacings. Our total level densities also fairly agree with the values extracted from the analysis of particle- γ coincidence in the $(^3\text{He},\alpha\gamma)$ and $(^3\text{He},^3\text{He}'\gamma)$ reactions, at least if normalized on the same density at the neutron binding energy. The combinatorial model has also been applied to estimate the NLD on top of the fission barriers and in the isomeric well. Finally, within the same framework, particle-hole NLD required for pre-equilibrium reaction models have been determined.

The final NLD (without renormalization on experimental data) are made available to the scientific community at the website <http://www-astro.ulb.ac.be>. The tables include the spin- and parity-dependent NLD for more than 8500 nuclei ranging from $Z=8$ to $Z=110$ for a large energy and spin grid ($U = 0$ to 200 MeV and the lowest 30 spins). No simple analytical fit to the tabulated NLD is given to avoid losing the specific microscopic characteristics of the model. It should be stressed that the combinatorial NLD cannot be approximated by a simple BSFG-type formula, except at very-high energies (above roughly 100 MeV), where the shell, pairing and deformation effects disappear.

The NLD have also been implemented in the TALYS reaction code (publicly available at <http://www.talys.eu>) where the normalization parameters entering Eq. 2 are also included. As we have shown, when experimental cross sections are available our normalization procedure globally improves the agreement with the data. Also, it is worth mentioning that the renormalization recipe is equivalent to what is usually done when one wants to fit cross sections by playing slightly with the usual level density parameters.

Still, some improvements may be required. In particular, the spherical/deformed character for transitional nuclei is not yet under control. In addition, at increasing energies, the shape of the nucleus changes, so that building the excitation configurations on top of the ground state single-particle properties may not be adequate. Such effects will be studied in a near future.

-
- [1] S. Hilaire and S. Goriely, Nucl. Phys. **A779** (2006) 63.
[2] A.C. Larsen et al., Phys. Rev. **C73** (2006) 064301 and references therein.
[3] H.A. Bethe, Phys. Rev. **50**, 332 (1936).
[4] A.J. Koning, S. Hilaire, S. Goriely, Nucl. Phys. **A810**, 13 (2008).
[5] S. Goriely, Nucl. Phys. **A605**, 28 (1996).
[6] A.V. Ignatyuk, IAEA report, INDC(CCP)-233/L (1985).
[7] A.V. Ignatyuk, IAEA report, TECDOC-1034, (1998).
[8] P. Decowski et al., Nucl. Phys. **A110**, 129 (1968).
[9] L.G. Moretto, Nucl. Phys. **A185**, 145 (1972).
[10] M. Hillman, J.R. Grover, Phys. Rev. **185**, 1303 (1968).
[11] S. Hilaire and J.P. Delaroche, *Nuclear Data for Science and Technology*, Italian Physical Society: Reffo et al. (eds), 1997, p. 694.
[12] S. Hilaire, J.P. Delaroche and A.J. Koning, Nucl. Phys. **A632**, 417 (1998).
[13] S. Hilaire, J.P. Delaroche and M. Girod, Eur. Phys. J. **A12**, 169 (2001).
[14] Y. Alhassid, S. Liu and H. Nakada, Phys. Rev. Lett. **83**, 4265 (1999).
[15] P. Demetriou and S. Goriely, Nucl. Phys. **A695**, 95 (2001).
[16] M. Sin et al., in *Nuclear Data for Science and Technology*, O. Bersillon et al (eds); EDP Sciences, (2008) p. 313.
[17] S. Goriely, S. Hilaire and A.J. Koning, Phys. Rev. **C78** (2008) 064307.
[18] Belgya T., Bersillon, O., Capote Noy, R. et al., *Handbook for calculations of nuclear reaction data, RIPL-2* (IAEA-Teedoc-1506), 2006.
[19] A. Schiller et al., Phys. Rev. **C63**, 021306 (2001).
[20] E. Melby et al., Phys. Rev. **C63**, 044309 (2001).
[21] A. Voinov et al., Phys. Rev. **C63**, 044313 (2001).
[22] S. Siem et al., Phys. Rev. **C65**, 044318 (2002).
[23] M. Guttormsen et al., Phys. Rev. **C63**, 064306 (2003).
[24] A. Schiller et al., Phys. Rev. **C68**, 054326 (2003).
[25] U. Agvaalvusan et al., Phys. Rev. **C70**, 054611 (2004).
[26] R. Chankova et al., Phys. Rev. **C73**, 034311 (2006).
[27] A.C. Larsen et al., Phys. Rev. **C73**, 064301 (2006).
[28] A.J. Koning, S. Hilaire, M.C. Duijvestijn, in *Nuclear Data for Science and Technology*, O. Bersillon et al (eds); EDP Sciences, (2008) p. 211.
[29] EXFOR library: <http://www-nds.iaea.or.at/exfor>.
[30] Z.Y. Bao, H. Beer, F. Käppeler, et al., At. Data Nucl. Data Tables **75**, 1 (2000).